1995AJ....110..856S

THE ASTRONOMICAL JOURNAL VOLUME 110, NUMBER 2 AUGUST 1995

COLLISIONAL TIME SCALES IN THE KUIPER DISK AND THEIR IMPLICATIONS

S. ALAN STERN

Geophysical, Astrophysical, and Planetary Sciences, Space Science Department, Southwest Research Institute, 1050 Walnut St. #429, Boulder, Colorado 80302

Electronic mail: alan@everest.space.swri.edu

Received 1995 February 15; revised 1995 May 1

ABSTRACT

We explore the rate of collisions among bodies in the present-day Kuiper Disk as a function the total mass and population size structure of the disk. We find that collisional evolution is an important evolutionary process in the disk as a whole, and indeed, that it is likely the dominant evolutionary process beyond $\approx$42 AU, where dynamical instability time scales exceed the age of the solar system. Two key findings we report from this modeling work are: (i) That unless the disk's population structure is sharply truncated for radii smaller than $\sim$1–2 km, collisions between comets and smaller debris are occurring so frequently in the disk, and with high enough velocities, that the small body (i.e., KM-class object) population in the disk has probably developed into a collisional cascade, thereby implying that the Kuiper Disk comets may not all be primordial, and (ii) that the rate of collisions of smaller bodies with larger $100<R<400$ km objects (like $1992QB_1$ and its cohorts) is so low that there appears to be a dilemma in explaining how QB_1's could have grown by binary accretion in the disk as we know it. Given these findings, it appears that either the present-day paradigm for the formation of Kuiper Disk is failed in some fundamental respect, or that the present-day disk is no longer representative of the ancient structure from which it evolved. This in turn suggests the intriguing possibility that the present-day Kuiper Disk evolved through a more erosional stage reminiscent of the disks around the stars β Pictorus, α PsA, and α Lyr. © *1995 American Astronomical Society.*

1. INTRODUCTION

Over the past few years, both the theoretical underpinnings and the observational evidence for a disk of comets and larger bodies beyond the orbit of Neptune has become increasingly secure (Jewitt & Luu 1995; Cochran *et al.* 1995). It now appears assured that the solar system possesses such a disk of material, and that this region is likely to contain the source population for the low-inclination, short-period, Jupiter Family Comets (Stern 1995a).

In this paper I explore the rate at which objects collide in the Kuiper Disk region. The basic rationale for such a study is rooted in the combination of a 10^3–10^4 times higher number density of comets and 10^1 times average orbital speed in the KD, compared to the Oort Cloud (Stern 1988), which together imply that collision rates should be 10^7–10^9 times higher in the Kuiper Disk. Further rationale is provided by analogy to the asteroid belt. The average surface mass density in the Kuiper Disk ($\sim10^{23}$–10^{24} g AU^{-2}) is similar to the value of $\sim3\times10^{23}$ g AU^{-2} in the asteroid belt, where collisions play an important and well-known evolutionary role. Even accounting for the $\sim$4 times lower random velocities at 40 AU in the Kuiper Disk (as opposed to 2 AU in the asteroid belt), the collisional intensity in the Disk (i.e., collisions cm^{-2} s^{-1} on a given target) is not very different from the asteroid belt.

Among the questions about the Kuiper Disk that one wishes to address with collision rate modeling are: What is the rate of collisions in the disk today? Is the Kuiper Disk collisionally evolved; that is, are cratering collisions an important surface modification process in the disk, and is the rate of collisions high enough to permit evolution in the size spectrum of bodies in the disk? Is it possible to constrain the properties of the ancient disk via collisional results? Is it possible to constrain the properties of the distant, as-yet undetected reaches of the disk via collisional results? And, are there detectable signatures of these collisions?

This paper represents an initial attack on several of these questions. It is organized as follows: In Sec. 2, I briefly review the evidence for the Kuiper Disk; Section 3 describes a model for computing collision rates in the present-day Kuiper Disk; Section 4 describes the results of model runs for the present-day Kuiper Disk; Section 5 examines the implications of these results; Section 6 explores whether collisions in the present-day disk promote accretion or erosion; Section 7 summarizes the results obtained in this paper and points out two significant inconsistencies between the collisional modeling results obtained here and the present understanding of the origin of objects in Kuiper Disk. Among the implications of the work reported here is that the present-day disk appears to be the remnant of a former disk with more mass, and very likely lower mean eccentricities, than observed today.

2. THE KUIPER DISK

Almost a half-century ago, Edgeworth (1949), and later Kuiper (1951), made prescient predictions that the Sun should be surrounded by a disklike ensemble of comets and other "debris" located beyond the orbit of Neptune. The case

© American Astronomical Society • Provided by the NASA Astrophysics Data System

1995AJ....110..856S

for such a primordial reservoir was strengthened when it was pointed out that such a disk could be an efficient source region to populate the low-inclination, short-period comets (Fernández 1980). Convincing dynamical simulations supporting this link between most short-period comets, and the Kuiper Disk (KD) region, first appeared when Duncan *et al.* (1988) and later Quinn *et al.* (1991) showed that a low-inclination source region appears to be required for the low-inclination orbit distribution of the Jupiter Family Comets. Figure 1 is a schematic diagram revealing the gross architecture of the disk in relationship to the orbits of the five known outer planets.

The computational capabilities available to Duncan and co-workers in the mid-1980s required some important approximations be accepted (for reviews of this work, cf. Weissman 1993, and Stern 1995a). These compromises were criticized by Bailey & Stagg (1990), but Duncan *et al.*'s work generated interest in the Kuiper Disk by both modelers and observers. Of particular relevance are the Holman & Wisdom (1993) and Levison & Duncan (1993) studies of orbital evolution in the disk. These two groups found a time-dependent dynamical erosion of the disk population inside ≈42 AU, caused by nonlinear perturbations from the giant planets. The dynamical chaos resulting from these perturbations is ultimately responsible for the transport of short-period comets from the long-lived Kuiper Disk reservoir to planet crossing orbits where they can be routinely detected. Based on the bias-corrected population of Jupiter Family comets and the dynamical transport efficiency of comets from the Kuiper Disk to the inner planets region, Duncan *et al.* (1995) have estimated that 6×10^9 comets orbit in the Disk between 30 and 50 AU from the Sun.

Observational confirmation of the Kuiper Disk was first achieved with the discovery of object $1992QB_1$ by Jewitt & Luu (1993). As of early 1994, no fewer than 25 QB_1-like, *trans*-Neptunian objects have been discovered (Jewitt & Luu 1995; Stern 1995a). These icy outer solar system bodies are expected to have dark surfaces consisting of an icy matrix contaminated by silicates and organics. Assuming a typical (i.e., cometary) geometric albedo of 4%, and the absence of coma, the distances and magnitudes of these objects indicate they have radii between roughly 50 and 180 km. Based on the detection statistics obtained to date, one can easily estimate that a complete ecliptic survey would reveal $\sim3.5\times10^4$ such bodies orbiting between ≈30 and 50 AU. Simple power-law extensions of this population predict a cometary population (which we define as bodies with radii between 1 and 6 km) of $\sim10^{10}$, which is similar to dynamical modeling results obtained by Duncan *et al.* (1995) to satisfy the short-period comet flux. Very recently, Cochran *et al.* (1995) have reported Hubble Space Telescope results giving the first direct evidence for comets in the Kuiper Disk.

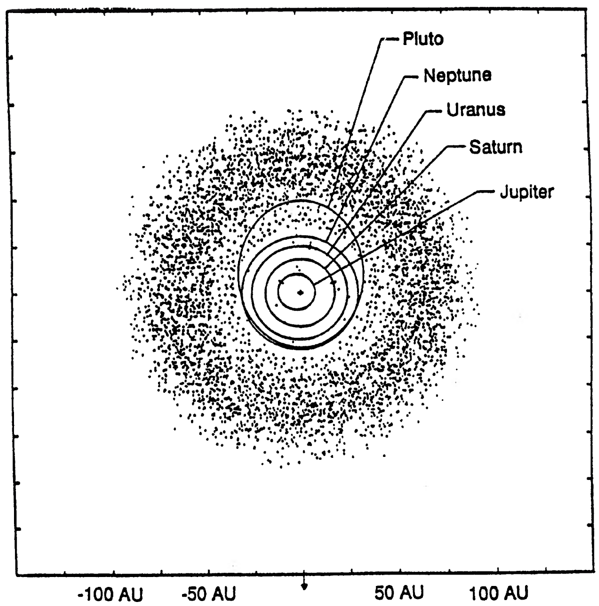

FIG. 1. Schematic depiction of the Kuiper Disk and the orbits of the outer planets, including Pluto. The clearing between the orbit of Neptune and the inner edge of the present day disk is created by the dynamical perturbations of the giant planets (cf. Holman & Wisdom 1993; Levison & Duncan 1993). The position of the outer boundary of the Kuiper Disk is not well constrained, and may well extend much farther than shown here.

3. COLLISION RATE MODELING

Our model for estimating collision rates in the Kuiper Disk begins by defining the Disk in terms of a power law exponent, α, on the size distribution of objects in the disk, so that the number of objects $dN(r)$ between radius r and $r+dr$ is given by

$$dN(r)=N_0 r^\alpha dr, \tag{1}$$

where N_0 is a normalization constant set by the estimated number of QB_1 objects. For the runs presented here, the bodies in each successive size bin r are a factor of 1.6 times larger in size (and equivalently, 4 times higher in mass). We *a priori* assume a size range beginning at $r=0.1$ km, and extending upward to $r=162$ km.

We also define a power law exponent β on the radial distribution of surface mass density $\Sigma(R)$ in the disk, so that

$$\Sigma(R)=\Sigma_0 R^\beta, \tag{2}$$

where Σ_0 is the normalization constant.

Once an input disk is defined as described above, the model bins the disk into a series of concentric tori that are 1 AU in radial width. For each radius bin/heliocentric bin pair, the model computes the collision rate a target will experience

TABLE 1. Collision model run cases.

Model	M_{disk} 30 AU < R <50 AU	Population Type	Disk Type	N_{QB1s} 30 AU < R <50 AU	N_{comets} 30 AU < R <50 AU
CSD 1e4 15	0.16 $M_\oplus$	NOM	CMB	36,461	9×10^9
CSD 1e4 25	0.12 $M_\oplus$	NOM	DMB	27,740	7×10^9
CSD 1e4 13	0.42 $M_\oplus$	CM	CMB	41,162	5×10^{10}
CSD 1e4 23	0.32 $M_\oplus$	CM	DMB	31,316	3×10^{10}
CSD 3e4 15	0.07 $M_\oplus$	NOM	CMB	17,950	4×10^9
CSD 1e6 13	12.3 $M_\oplus$	CM	CMB	1.2×10^6	1.3×10^{12}

Notes to TABLE 1

$\mathcal{M}_{disk}$ is the integral mass over all size bins. CMB=constant mass per radial bin ($\beta=-1$); DMB=constant mass per radial bin ($\beta=-2$). NOM=Nominal mass per size bin ($\alpha=-11/3$); CM=constant mass per size bin ($\alpha=-4$).

© American Astronomical Society • Provided by the NASA Astrophysics Data System

1995AJ....110..856S

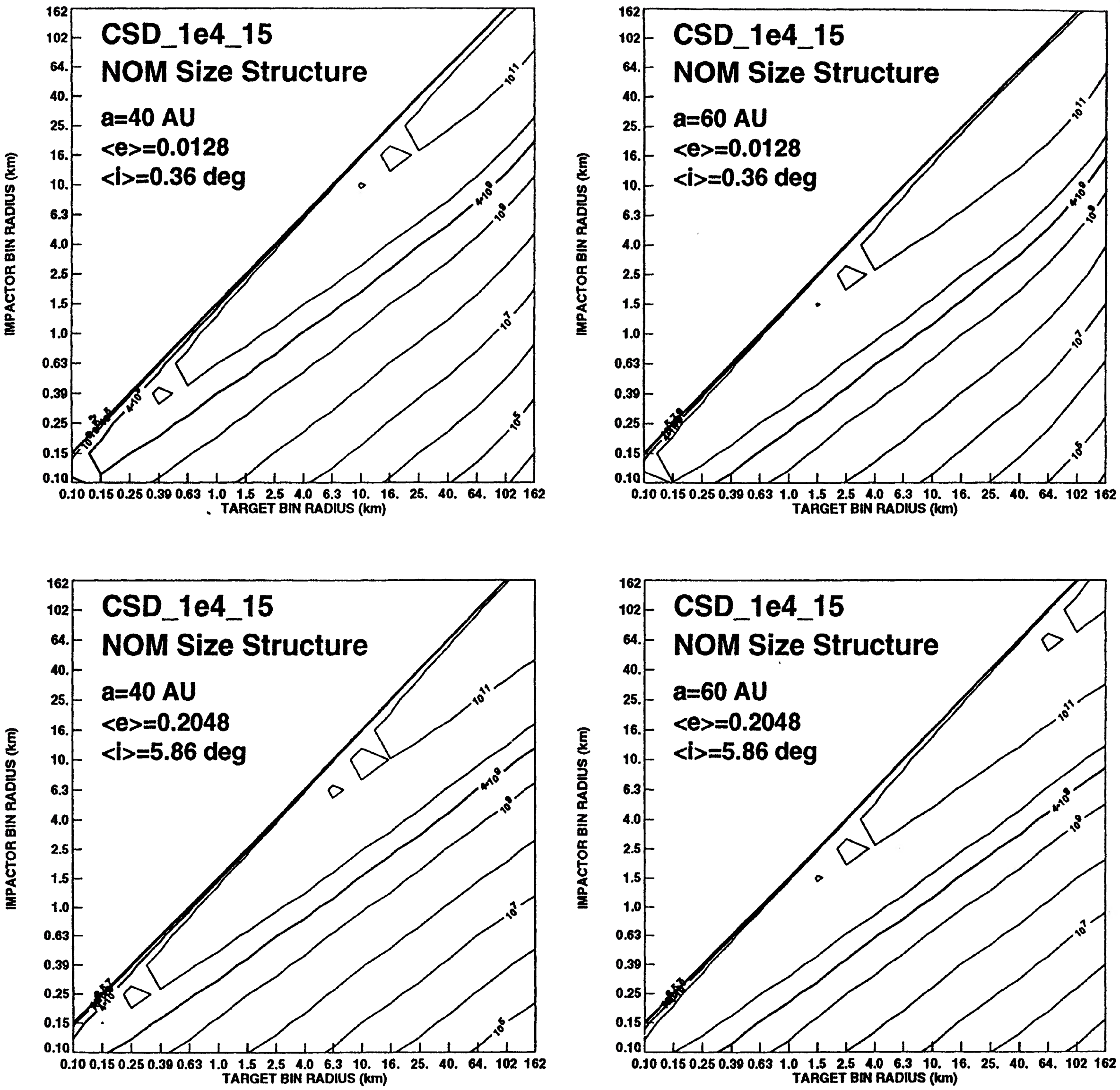

FIG. 2. Contours of the collision time scales (in years) at two locations in the Kuiper Disk (40 and 60 AU), as a function of target and impactor size for the model run with a constant mass per heliocentric bin (CMB) and a "nominal" size structure. The upper panels are for a disk with $\langle e\rangle \approx 0.01$; the lower panels are for a disk with $\langle e\rangle \approx 0.20$.

from objects in all bins of equal or smaller size. This is of course a function of $\langle e\rangle$, since $\langle e\rangle$ controls both the internal velocity dispersion in the disk, as well as the degree of heliocentric bin crossing. In what follows we assume $\langle i\rangle = \frac{1}{2}\langle e\rangle$. Because there is presently no information on the way in which ensemble-averaged inclinations ($\langle i\rangle$) and eccentricities ($\langle e\rangle$) vary in the Kuiper Disk, we adopt a disk-wide $\langle i\rangle$ and $\langle e\rangle$ for each run, and vary these quantities from run to run as free parameters to explore how sensitive the model results are to these variables.

Collisions are not allowed outside the boundaries of the disk, so in the case of moderate or high eccentricity orbits, objects can spend significant time in "open" space outside the disk where collisions are not allowed to occur. This creates edge effects, but such effects may actually occur if the disk in fact sharply truncates at its boundaries.

To compute collision rates we adopt a particle in a box formalism. In this approach, the instantaneous collision rate c of objects with semimajor axis a, eccentricity e, and radius r_x being struck by objects of radius r_y is

$$c(r_x, r_y, a, e) = n\sigma_g v, \tag{3a}$$

where n is the local space density of impactors, v, is the local average crossing velocity of the target body against the KD population at distance R, and σ_g is the collision cross section of the impactor+target pair, corrected for gravitational focusing. Gravitational focusing is an important correction for targets in the QB_1 size range and larger, particularly in the case of very low disk eccentricities (e.g., $\langle e\rangle < 10^{-2}$). The orbit-averaged collision rate $\bar{c}(r_x, r_y, a, e)$

© American Astronomical Society • Provided by the NASA Astrophysics Data System

1995AJ....110..856S

can be written to show its implicit dependencies in the model as:

$$\bar{c}(r_x,r_y,a,e)=\sum_{R=a(1-\langle e\rangle)}^{a(1+\langle e\rangle)} f(a,\langle e\rangle,R)n(r_y,R)\times v_{xy}(a,\langle e\rangle,\langle i\rangle,R)\sigma_g(r_x,r_y,v_{xy},v_{\mathrm{esc}(x+y)}). \tag{3b}$$

Here the term f represents the ratio of $T(a,\langle e\rangle,R)$, the time the target body in an orbit defined by $(a,\langle e\rangle,\langle i\rangle)$ spends in each torus it crosses during its orbit, to this target's orbital period, $(4\pi^2a^3/GM_\odot)^{1/2}$.

To compute $T(a,\langle e\rangle,R$, I solve the central-field Kepler time of flight equation explicitly for every $(a,\langle e\rangle)$ pair in the run parameter space. The number density of impactors $n(r_y,R)$ in the torus centered at distance R is computed from the defining mass of the disk, its wedge angle $\langle i\rangle$, its radial surface density power law, and the population size structure power law.

To compute the average crossing velocity of the impactor population on the target body when the target is in the bin at heliocentric distance R, we use

$$v_{xy}=v_K(a)\sqrt{2\langle e\rangle^2+2\langle i\rangle^2-3\left(\frac{a-R}{a+R}\right)^2} \tag{4}$$

(Petit & Hénon 1987), where v_K is the average Keplerian orbital speed of the target body, and the term under the radical is the relative velocity correction for crossing orbits. The collision cross section σ_g is computed according to

$$\sigma_g=\pi(r_x+r_y)^2\left[1+\frac{2G(m_x+m_y)}{v_{xy}^2(r_x+r_y)}\right], \tag{5}$$

where the term in brackets adjusts for gravitational focusing. To compute masses from radii I assume a density of 1 g cm^{-3}.

As a result of these calculations and the nested loops in a,r_x, and r_y, the model produces an array of collision rates $\bar{c}(r_x,r_y,a,e)$ throughout the specified disk, where the free parameters defining the disk are the total number of QB_1's interior to 50 AU, α, β, and $\langle e\rangle$. From this array the model computes subsidiary quantities such as the mean time between collisions $\tau(r_x,r_y,a,e)$,

$$\tau(r_x,r_y,a,e)=\bar{c}^{-1}(r_x,r_y,a,e), \tag{6}$$

the mass impact rate from all impactors on each target size class:

$$\dot{M}(r_x,a,e)=\sum_{r_y=r_{\min}}^{r_x}\bar{c}(r_x,r_y,a,e)m(r_y), \tag{7}$$

and the total collision rate on entire population in each target size bin:

$$\bar{C}(r_x,a,e)=\sum_{r_y=r_{\min}}^{r_x}\bar{c}(r_x,r_y,a,e)N(r_x,a), \tag{8}$$

where $N(r_x,a)$ is the population of targets of radius r_x with semimajor axis a. We also compute a characteristic time for growth, τ_G, as

$$\tau_G(r_x,a,e)=\frac{M(r_x,a)}{\eta\dot{M}(r_x,a,e)}, \tag{9}$$

where η is the mass accretion efficiency per collision.

4. MODEL INPUT PARAMETERS

In the runs presented below, I assume a disk inner radius of 35 AU and an outer radius of 70 AU. I let eccentricity range as a free parameter from 1×10^{-4} to 2×10^{-1}, which extends over the range of detected eccentricites of QB_1 objects detected to date (Jewitt & Luu 1995; H. Levison, personal communication 1995). As noted above, I assume the equilibrium condition $\langle i\rangle=\frac{1}{2}\langle e\rangle$.

Four cases defining the radial mass dependence and size distribution of objects in the disk have been studied. These four cases represent the various combinations of two radial mass distributions [cf., α in Eq. (1)] and two size distributions [cf., β in Eq. (2)].

For the radial distribution of mass in the disk, the two cases we run are defined as follows One case assumes a constant mass per radial bin (CMB; $\alpha=-1$), which corresponds to a surface mass density that declines with heliocentric distance as R^{-1}. The second, and more realistic case, assumes a declining mass per bin (DMB; $\alpha=-2$), corresponding to a surface mass density falling like R^{-2}. These two cases bracket the realistic range of parameter space (Lissauer 1987).

Concerning the size distribution of objects in the disk population, the model grid allows for 17 size bins, each a factor of 1.6 larger in radius. We assume a minimum radius for KD impactors of 0.1 km. This results in an upper size limit of $r=162$ km, which is consistent with the largest detected bodies among the QB_1 population. Our favored size distribution, which we call the nominal (NOM) case, connects the observationally estimated $\sim3.5\times10^4$ QB_1-sized objects (Jewitt & Luu 1995) inside 50 AU with the modeling-derived estimates of $\sim10^{10}$ comets (Duncan *et al.* 1995) in a single power law with $\alpha=-11/3$. Our second case assumes $\alpha=-4$, which gives a constant mass in every logarithmic size bin; this case is called the CM case. Relative to the NOM case which produces $\approx10^{10}$ for 35,000 QB_1's (100 km in radius or larger), the CM case produces $\approx5\times10^{10}$ comets.

Table I summarizes some the important attributes of these four run cases, as well as two additional run cases described in Secs. 6 and 7. With these preliminaries described, we now discuss the results relating to these four model cases.

5. MODEL RESULTS: COLLISION AND GROWTH TIME SCALES

Figures 2 and 3 depict the collision time scale results obtained using the model described in Secs. 3 and 4. Results are presented at two heliocentric distances, 40 AU (on the left) and 60 AU (on the right). In each figure, the upper panels show the collision time scale for $\langle e\rangle\approx10^{-2}$, and the lower panels show the collision time scale for $\langle e\rangle\approx2\times10^{-1}$. These values of $\langle e\rangle$ bound the measured eccentricity of all Kuiper Disk objects with known eccentricities. Similar data

© American Astronomical Society • Provided by the NASA Astrophysics Data System

1995AJ....110..856S

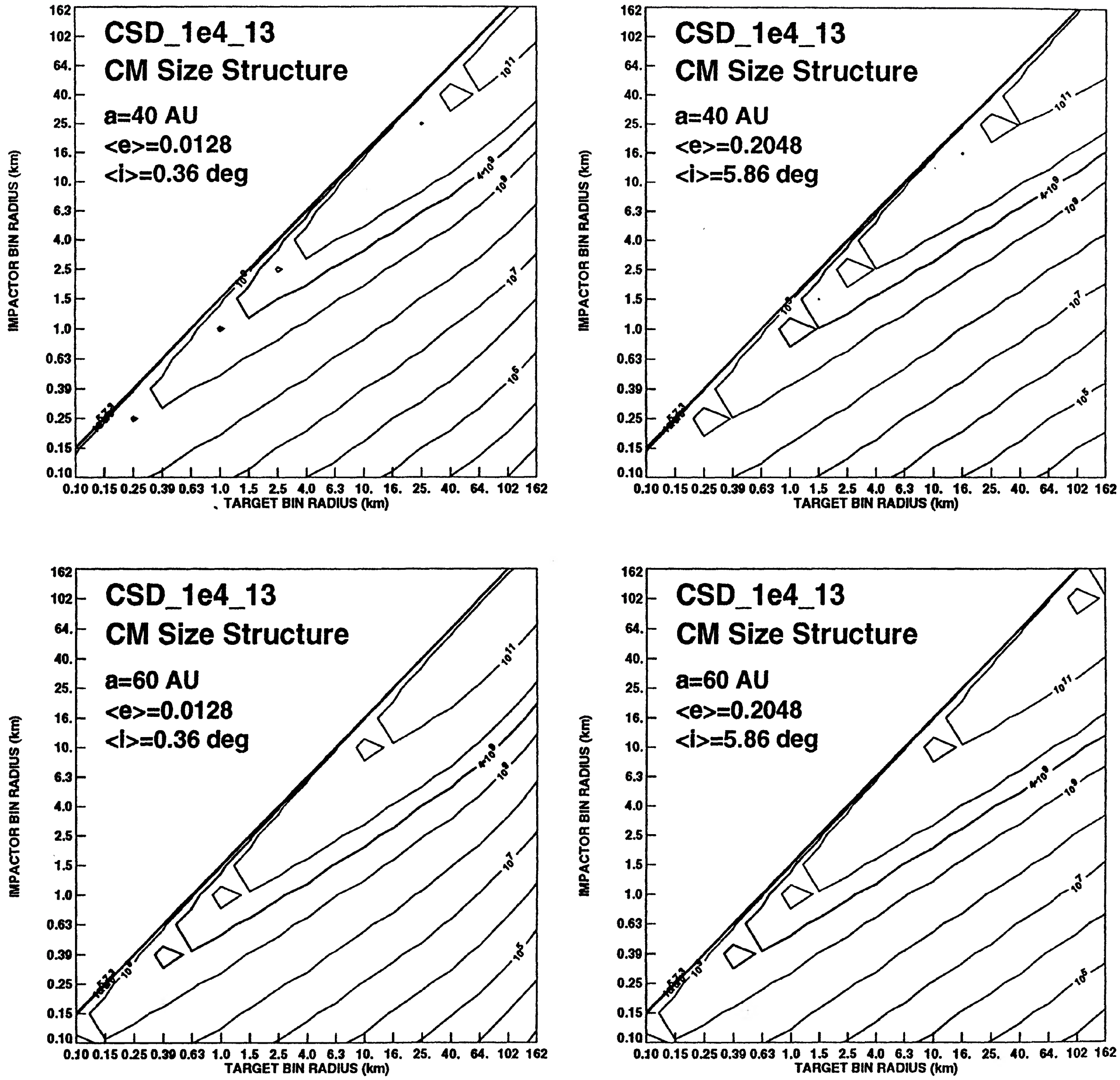

FIG. 3. Contours of the collision time scales (in years) at two locations in the Kuiper Disk (40 and 60 AU), as a function of target and impactor size for the model run with a constant mass per heliocentric bin (CMB) and constant mass (CM) per bin size structure. The upper panels are for a disk with $\langle e\rangle \approx 0.01$; the lower panels are for a disk with $\langle e\rangle \approx 0.20$.

that have been computed for the two DMB ($\Sigma \sim R^{-2}$) cases are not shown because the results are not significantly different.

These data can be used to ascertain a number of interesting facts about collisions in the present-day disk. Two results that are relevant to our later discussions concern the following.

(1) *Collisional Time scales on Comets in the Disk:* We define a "comet" as those disk objects in the radii bins from 1 to 6 km. In the case of the NOM population structure (cf., Fig. 2), the largest impactor a comet at 40 AU typically collides with in 4×10^9 yr has a radius $\approx$5 times smaller than the comet itself; at 60 AU the largest impactor on a comet is typically $\approx$10 times smaller. In the case of a CM population structure (cf., Fig. 3), which has more small bodies and therefore shorter collisional time scales than the nominal-case population, comets are expected to be struck by approximately like-sized impactors at 40 AU, and 2.5 times smaller objects at 60 AU. And,

(2) *Collisional Time scales on QB_1 Bodies:* We define "QB_1 bodies" to be objects in the 102 and 162 km radius bins, which span essentially the range of detected QB_1 radii (see, e.g., Jewitt & Luu 1995). Notice in Figs. 2 and 3 that over the age of the solar system, the largest impactor on a typical QB_1 body will be $\approx$6–16 km in radius, depending on the population structure and eccentricity of the disk. Notice also that each QB_1 object will suffer a cratering collision with a km-class object every 10^6–10^7 yr in a CM population and every $\sim10^7$–10^8 yr in the NOM population. Among the entire population of $\sim3.5\times10^4$ QB_1 bodies inside $\sim$50 AU,

© American Astronomical Society • Provided by the NASA Astrophysics Data System

1995AJ....110..856S

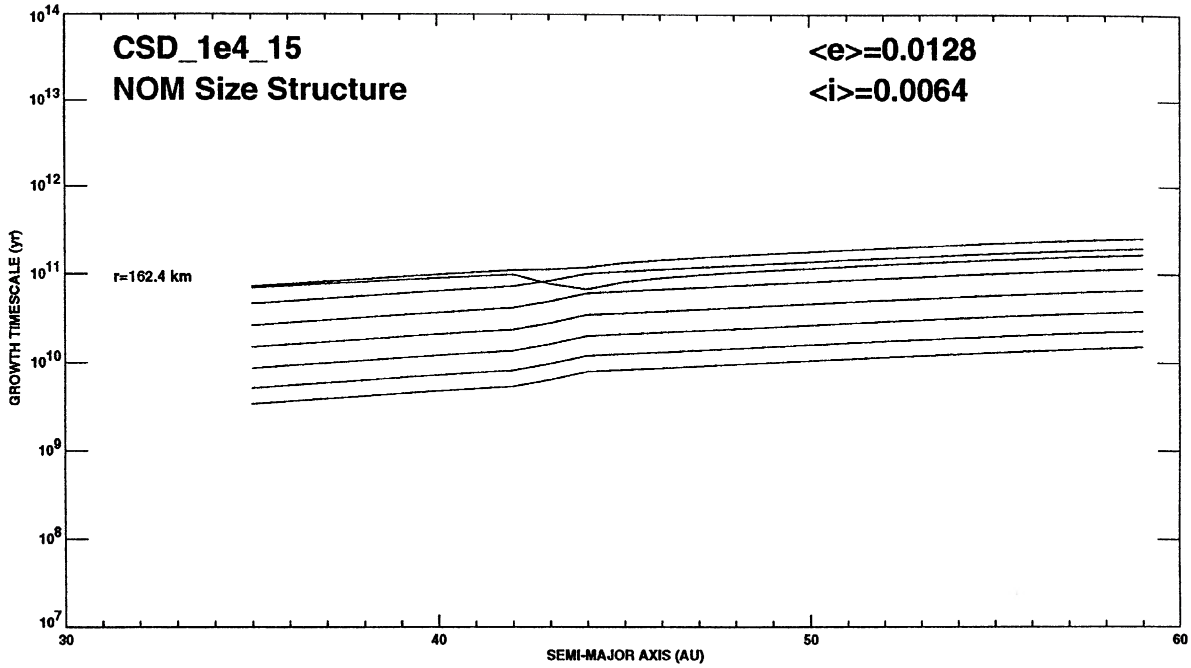

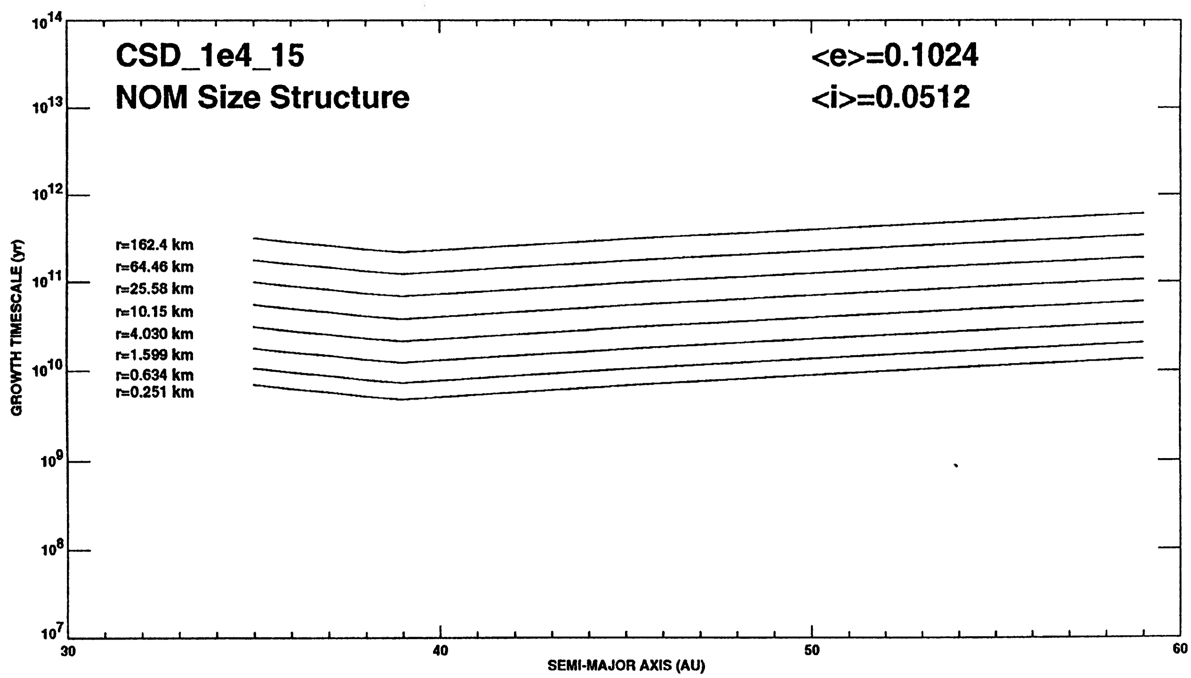

FIG. 4. Lower limit growth time scales as a function of target size and heliocentric distance for the model run with a Constant Mass per heliocentric bin (CMB) and a nominal size structure.

one expects $\sim 10^2-10^3$ collisions with a km-class objects every year, depending on whether the population structure is more like the NOM or CM case. These collision rates suggest that although impacts on individual objects occur infrequently, the population ensemble produces collisions frequently. This in turn suggests that a significant amount of dust may be injected into the Kuiper Disk every year, possibly leading to detectable signatures. This subject is beyond the scope of this paper, but is thoroughly investigated elsewhere (cf., Stern 1995b).

The results presented in Figs. 2 and 3 demonstrate very clearly that both small and large objects in the Kuiper Disk suffer collisions on time scales much shorter than the age of the solar system.

It is next crucial to ask whether present-day rate of colli-

© American Astronomical Society • Provided by the NASA Astrophysics Data System

1995AJ....110..856S

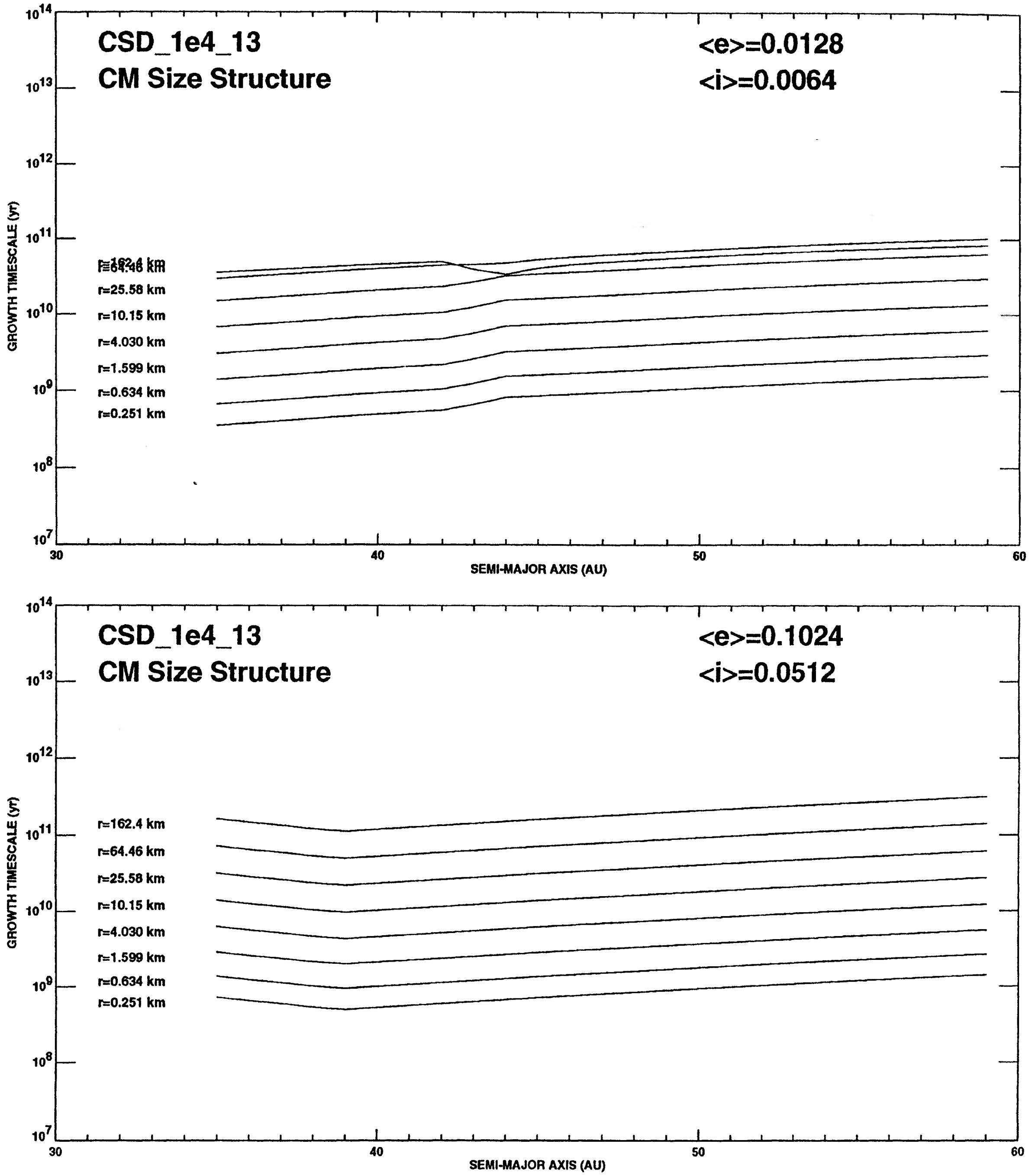

FIG. 5. Lower limit growth timescales as a function of target size as heliocentric distance for the model run with a Constant Mass per heliocentric bin (CMB) and constant mass (CM) per bin size structure.

sions is large enough to have built the largest (i.e., QB_1) bodies we see in the disk. To address this question I have computed growth times using the formalism imbedded in Eq. (9), with the assumption that the growth efficiency factor (i.e., the mass accreted divided by mass incident) is unity. With $\eta=1$, collisions are completely inelastic. This is physically unrealistic, since many collisions will result in erosion of the target rather than net accretion; however, it provides a useful *lower limit* to the actual growth times. As we shall see, even the lower limit QB_1 growth times are longer than the age of the solar system.

Figures 4 and 5 depict the results of such lower-limit growth time calculations for the same two model runs that produced the collision time scales in Figs. 2 and 3, respectively.

The results shown in Figs. 4 and 5 can be summarized as follows. For both the NOM and CM population size structures, collisions are so infrequent that even km-scale bodies

© American Astronomical Society • Provided by the NASA Astrophysics Data System

1995AJ....110..856S

cannot not accrete their own mass in the age of the solar system, even if every collision is perfectly accretional (i.e., inelastic). In the case of the CM population structure, the largest objects that can be grown in 4×10^9 yr are only a few km in radius.

These results are not a strong function of $\langle e\rangle$ if $\langle e\rangle > 0.01$, as appears to be the case in the present-day disk. *As a result, we must conclude that binary accretion in the present day disk cannot explain the growth of QB_1-class bodies on time scales less than about an order of magnitude longer than the age of the solar system.* The implications of this finding will be discussed in more detail in Sec. 7.

6. ECCENTRICITIES FOR GROWTH AND EROSION

Up to this point we have not been strongly concerned with the issue of whether collisions in the KD promote communition or growth. Instead we have been satisfied to simply count collisions and compute time scales. We have seen that binary collisions are too infrequent to explain the growth of objects larger than a few km in radius, even if all collisions promote growth. Now we explore whether growth can take place at all, or whether instead the collisions promote erosion.

Whether a given collision between an impactor and a target results in growth or erosion depends primarily on the energy of the impact. In the Kuiper Disk a typical approach velocity of two objects at a distance large compared to the Hill sphere of the target can be reasonably-well approximated by

$$v_\infty = \sqrt{2}v_K(\langle e^2\rangle + \langle i^2\rangle)^{1/2}, \tag{10}$$

where v_K is the local Keplerian velocity. For the standard assumption that $\langle i\rangle = \frac{1}{2}\langle e\rangle$, we have,

$$v_\infty = \sqrt{3}\langle e^2\rangle^{1/2} v_K. \tag{11}$$

The energy at impact is therefore given by

$$\tfrac{1}{2}\mu v_{\rm imp}^2 = \tfrac{1}{2}\mu(v_{\rm esc} + \sqrt{3}\langle e^2\rangle^{1/2} v_k)^2, \tag{12}$$

where μ is the reduced mass and $v_{\rm esc}$ is the escape velocity of the two colliding bodies measured at the radius of impact. The critical velocity for net erosion to occur is given by the requirement that the specific impact energy must exceed the combined energy lost (a) to dissipation, (b) to break up the surface, and then (c) to disperse the ejecta out of the gravitational well of the combined mass of the impactor/target collision pair. The impact energy, $E_{\rm imp}$, as given by Eq. (12), must equal or exceed these energy sinks; if it does not, the target will accrete some mass in the collision. The critical condition for the target to lose mass occurs when the mass of the ejecta exceeds the mass of the impactor. Therefore, if the impactor mass is small compared to the target, we require

$$\tfrac{1}{2} v_{\rm imp}^2 > \kappa(v_s^2 + \tfrac{1}{2} v_{\rm sec}^2), \tag{13}$$

where v_s represents the velocity required to mechanically shatter the target surface, $v_{\rm esc}$ represents the velocity required to disperse the debris to infinity, and κ is a factor that takes into account energy losses partitioned into heat, sublimation, hydrodynamic effects, and other factors. We take the specific energy for mechanical breakup of the target surface to be

$$v_s = \sqrt{s}, \tag{14}$$

where s is the specific strength of the target material at zero compression. And of course the escape velocity is given by

$$v_{\rm esc} = \sqrt{\frac{2GM_t}{r_t}}, \tag{15}$$

where G is the universal gravitational constant, M_t is the combined mass of the target and impactor, and r_t is the combined radii of these two objects. From Eqs. (9)–(15) one can derive the condition which we must solve for:

$$v_{\rm esc}^2 + 2\sqrt{(3)}e^* v_K v_{\rm esc} + 3(e^*)^2 v_K^2 - \kappa v_s^2 - \kappa v_{\rm ej}^2 = 0, \tag{16}$$

to obtain e^*, the critical eccentricity at which impact energies are high enough to promote net erosion. Notice e^* is a function of several parameters, including the target strength, size, and mass, as well as the heliocentric distance.

TABLE 2. Critical eccentricities (e^*) for erosion.

Target Radius	35 AU (Strong)	60 AU (Strong)	35 AU (Weak)	60 AU (Weak)
001 km	7×10^{-3}	9×10^{-3}	1×10^{-3}	1×10^{-3}
010 km	6×10^{-3}	7×10^{-3}	2×10^{-3}	3×10^{-3}
100 km	5×10^{-2}	6×10^{-2}	2×10^{-2}	3×10^{-2}
170 km	9×10^{-2}	1×10^{-1}	4×10^{-2}	5×10^{-2}

Notes to TABLE 2

Strong implies $\rho=2$ g cm^{-3} and $s=3\times10^6$ erg g^{-1}; weak implies $\rho=0.5$ g cm^{-3} and $s=3\times10^4$ erg g^{-1}. In both cases we take $\kappa=8$ and $v_{\rm ej}=0.20v_{\rm esc}$ (e.g., Davis *et al.* 1989); see Sec. 6 for additional details.

Table 2 gives solutions to Eq. (16) for the critical erosion eccentricity e^*, both for impacts onto strong (e.g., rock/ice) targets ($\rho=2$ g cm^{-3} and $s=3\times10^6$ erg g^{-1}), and relatively weak (e.g., snowlike) targets ($\rho=0.5$ g cm^{-3} and $s=3\times10^4$ erg g^{-1}) at heliocentric distances of 35 and 60 AU. Following the results discussed in Fujiwara *et al.* (1989), we assume $v_{\rm ej}=0.2v_{\rm imp}$ and $\kappa=8$.

The results presented in Table 2 show that e^* for QB_1-sized targets with radii near 100 km, $e^*\geqslant0.02-0.03$ is required for net erosion if they are weak, and $e^*\geqslant0.05-0.06$ is required if they are strong. Similarly, for QB_1-like objects with $R=170$ km, which is comparable to the largest-discovered objects in the disk to date, $e^*\geqslant0.04-0.05$ is required to result in net erosion if the objects are weak, and $e^*\geqslant0.09-0.10$ is required if the objects are strong. For reference, at 35 AU an $\langle e\rangle=0.01$ corresponds to a typical encounter velocity at infinity of 87 m/s. We conclude from these results and the orbits of objects detected to date that some QB_1's should be undergoing erosion, while others may be in an accretional regime, depending on their eccentricity and strength. However, it is worthwhile to note that if the characteristic ejecta velocity v_{ej} is as low as a few percent of the impact speeds $v_{\rm imp}$, then e^* will rise dramatically and the QB_1 population will be in an accretional mode, even for eccentricities as high as 0.2–0.5. Unfortunately, until much better eccentricity statistics become available, it is not possible to determine if the QB_1 population as a whole is gaining or losing mass. All we can say is that the range of de-

© American Astronomical Society • Provided by the NASA Astrophysics Data System

1995AJ....110..856S

tected eccentricities spans the range of e^*'s, creating a complex situation.

The results presented in Table 2 show that e^* for comets is in the neighborhood of 10^{-3} to 10^{-2}, depending in large part on the true strength of comets. These results remain valid even if the characteristic ejecta velocity is as low as 5% of the impact speed, instead of 20%, as assumed in Table 2. This result and the fact that cometary orbit inclinations in the disk appear to be like QB_1 inclinations, imply that collisions on comets today are erosive. This finding also indicates that a collisional cascade is probably taking place among the small bodies in the Kuiper Disk. As pointed out by P. Farinella (personal communication 1995), this finding strengthens the analogy made in Sec. 1 between the Kuiper Disk and asteroid belt collisional regimes.

To determine how much mass a typical comet will loose in the age of the solar system, we combine the collision time scales in Figs. 2 and 3 with the algorithm outlined in Eqs. (10)–(16) to calculate a characteristic time scale $(M/\dot{M})$ for such objects to erode to zero mass. This is accomplished through a numerical code, which we point out, only allows mass loss when $e>e^*$. With this code, we find that between 35 and 55 AU, the critical size for catastrophic (i.e., complete) erosion is $\approx$1–2 km, depending on the properties of the target and the disk population structure. In addition, we find that comets perhaps as large as 4 km in radius can exhibit erosion timescales shorter than the age of the solar system inside $\approx$40 AU, if $\langle e\rangle>0.04$.

To support these conclusions, Fig. 6 shows a set of erosion time scales calculated for a mechanically strong (i.e., $s=3\times10^6$ erg g^{-1}) comet 1 km in radius, assuming $v_{ej}=0.1v_{imp}$. The impact time scales used in this calculation were from the Fig. 2 dataset. Figure 6 shows that throughout the region from 35 to 55 AU, the erosion time for such bodies is less than or equal to the age of the solar system. These erosion time scales will be further shortened if either comets are weaker than assumed in Fig. 6 (as is likely), or if the characteristic ejecta velocity v_{ej} is a smaller fraction of the impact velocity (which is quite possible). Substituting the collision statistics developed in the run for Fig. 3 marginally increases the erosion times over what is shown in Fig. 6, but does not materially affect our conclusions.

Therefore, unless the population of sub-km objects (which dominate the collision rates on comets in our model) was severely depleted below that predicted by the NOM and CM power laws, these results imply (i) that objects with radii $\sim$1–2 km and smaller are probably not mechanically primordial and (ii) that a change in the slope of the size distribution probably occurs for radii below $\sim$2–4 km. Depending on the slope structure of the primordial KD population power law, it may also be that the present-day disk contains far fewer comets than in the distant past.

One factor that could stymie the collisional cascade among small bodies in the $\sim$30–60 AU region of Kuiper Disk would be a sharp cutoff in the number of small bodies. The recent detection of comets in the 40 AU region by Cochran *et al.* (1995) provides strong evidence that any such cutoff must occur below the *HST* detection threshold, which corresponds to a radius near 6 km. To test this hypothesis, another run was made using the fifth disk input case shown in Table 2. In this run, the population of bodies in the Kuiper Disk was fully truncated below 1 km. As shown in Fig. 7, the resulting survival time scales against erosion for 1 km objects increase to much longer than the age of the solar system, even for eccentricities as high as 20%. As such, it can be concluded that the collisional cascade indicated by the results shown in Fig. 6 can be prevented if the Kuiper Disk population is somehow severely truncated below 1 km. If this is in fact the situation in the disk today, then it implies that either the number of sub-km KD bodies has always been severely depleted (i.e., there was a primordial size cutoff below 1 km), or that this condition arose through subsequent collisional evolution.

Whether in fact collisions caused a depletion of sub-km sized objects to develop, or as may be more likely, collisions have created a collisional cascade to develop at sizes around a few km and less, two facts remain clear: First, collisional evolution has played a key role in shaping the population structure of the Kuiper Disk we observe today. And, second, that the signature of this collisional evolution should reveal itself in a distinct break in the population structure of the Kuiper Disk for objects with radii somewhere between $\sim$1 and $\sim$6 km.

7. SUMMARY AND DISCUSSION

The results obtained in this paper provide strong evidence that collisions have been an important evolutionary mechanism in the Kuiper Disk. Indeed, because the dynamical instability time in the disk beyond $\approx$42 AU exceeds the age of the solar system (e.g., Levison & Duncan 1993; Duncan *et al.* 1995; Morbidelli *et al.* 1995), collisions appear to be the dominant evolutionary mechanism in the disk, at least inside 60 AU.

The most important results obtained from the first-generation collision model described in this paper are as follows.

(1) That the total rate of collisions of smaller bodies with QB_1-class objects is so small that there appears to be a dilemma in explaining how QB_1's could have grown by binary accretion in the disk as we know it.
(2) That present-day eccentricities in the disk preferentially promote erosion over accumulation for objects a few km in radius and smaller.
(3) As a result, it appears that either the population of objects smaller than $\sim$1 km in radius was originally deficient, or the present-day population structure of the Disk is involved in a collisional cascade; if that later is the case, then many Kuiper Disk comets may not be structurally primordial. And,
(4) That, owing to the frequency and energetics of collisions between several-km class and smaller bodies, a distinct break in the population structure of the Kuiper Disk likely occurs for objects with radii somewhere between $\sim$1 and $\sim$6 km.

© American Astronomical Society • Provided by the NASA Astrophysics Data System

1995AJ....110..856S

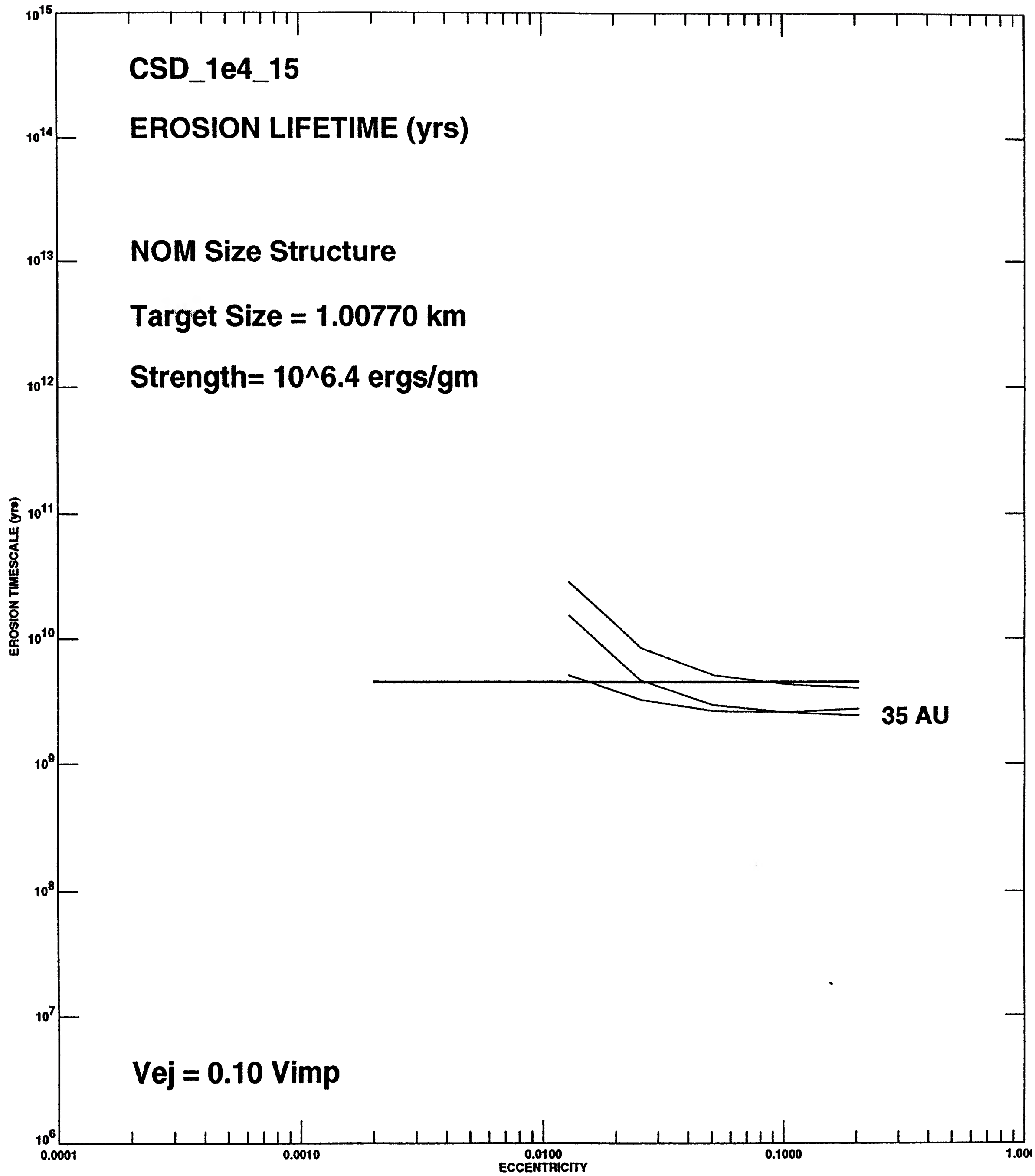

FIG. 6. The time scale against erosion for 1 km radius objects at 35, 45, and 55 AU in the NOM/ CMB case, as a function of their $\langle e \rangle$, compared to the age of the solar system (shown as the horizontal bar). Both weaker and smaller objects erode even more rapidly.

Conclusion (1) is particularly important. Simply put, it implies that collisions appear to be too infrequent to accumulate QB_1-sized objects in anything approaching the age of the solar system. This appears to provide evidence that either the mass and population structure of the Kuiper Disk have strongly evolved over time, or that large objects like the QB_1's were not built via the aufbau (i.e., "building up") process of binary accretion.

Together, findings (1)–(3) strongly suggest that something fundamental is missing in our present state of knowledge about the Kuiper Disk. One possibility is that the QB_1-class bodies were formed directly from the nebula, rather than by binary accretion of smaller objects. Alternatively, two possibilities based on the temporal evolution of the Disk suggest themselves.

First, it may be that the mass of solids in the disk was

© American Astronomical Society • Provided by the NASA Astrophysics Data System

1995AJ....110..856S

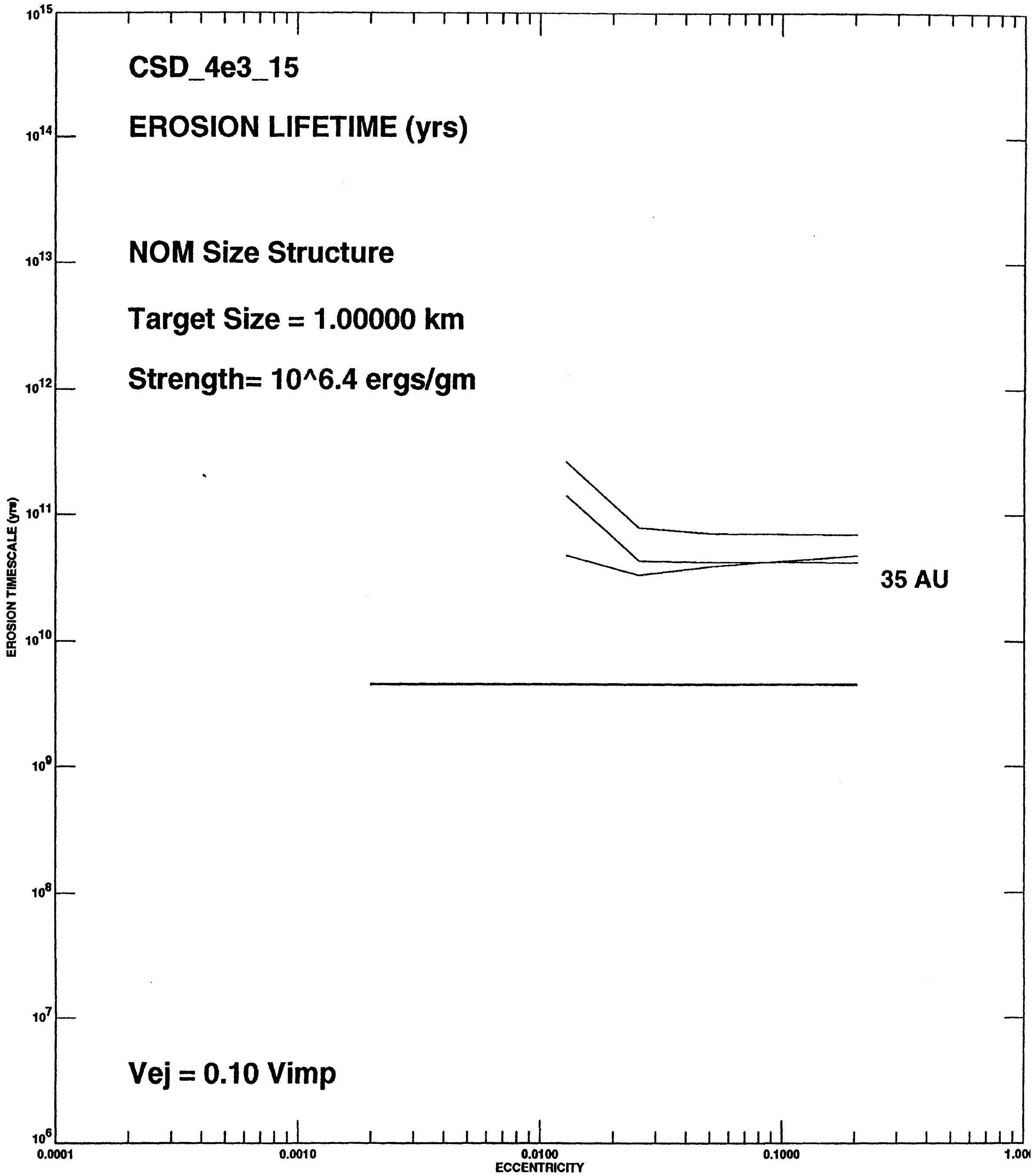

FIG. 7. Erosion time scales at 35, 45, and 55 AU in the Kuiper Disk, as a function of $\langle e \rangle$, for the final collision run case shown in Table 1. In this case the population structure is truncated for objects with radii <1 km. With the population truncated this way, cometary bodies suffer fewer collisions and therefore easily survive for longer than the age of the solar system, even for eccentricities high enough to promote erosion.

much higher in the past than in the present. A higher mass and therefore a higher mass density would have promoted faster growth of QB_1 bodies. The upper panel in Fig. 8 shows the lower-limit growth times for such a case, with $\mathcal{M}_{\rm disk}=12.3\mathcal{M}_{\oplus}$. This disk mass would be consistent with a continuation from 30 to 60 AU of the rather smooth surface mass density power law for solid material that extends from Jupiter to Neptune, but is today truncated at 30 AU. The lower panel in Fig. 8 clearly shows that "restoring the missing mass" in the 30–60 AU zone does indeed reduce the lower limit to QB_1 growth times sufficiently. However, because collisions between small bodies would still be erosional in a higher mass disk with such $\langle e \rangle$'s, adding mass to the KD region is not (alone) sufficient to solve the QB_1 dilemma.

Much lower eccentricities could provide a remedy, how-

© American Astronomical Society • Provided by the NASA Astrophysics Data System

1995AJ....110..856S

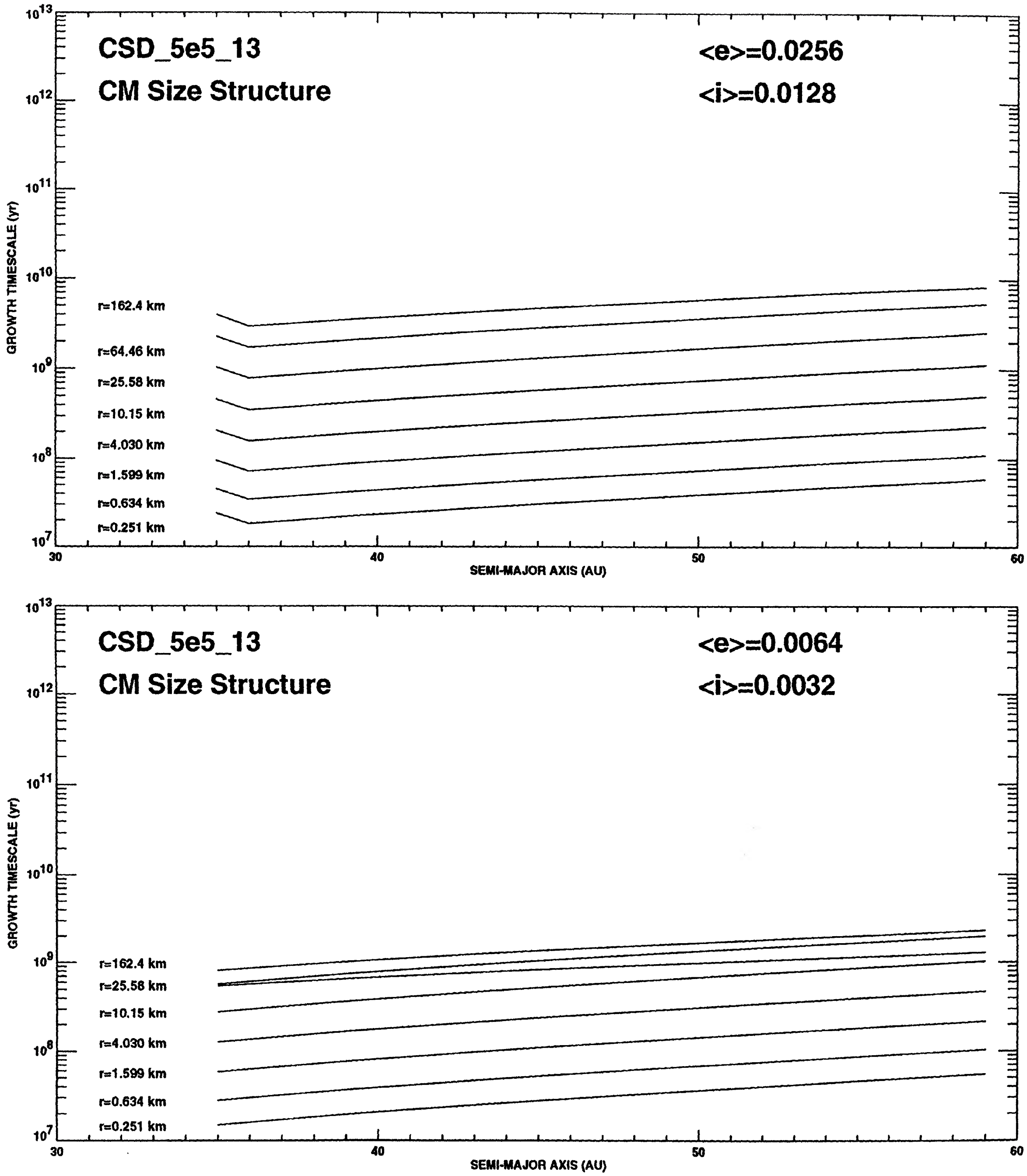

FIG. 8. The lower limit growth time scales in a 12.3 $\mathscr{M}_\oplus$ disk with $\langle e\rangle \approx 3\times10^{-2}$ (upper panel) and $\approx 6\times10^{-3}$ (lower panel). The data in the upper panel demonstrate the effectiveness of increasing the disk mass, as a means of growing QB_1 bodies in less than the age of the solar system in a disk with a mean eccentricity of up to 3%. Calculations not shown here demonstrate that further increasing the disk mass to $\sim 30\mathscr{M}_\oplus$ makes growth at $\langle e\rangle = 10^{-1}$ feasible. However, as described in Secs. 6 and 7, eccentricities below $\approx 1\%$ are required to permit km-class bodies to grow. The lower panel shows growth time scales in the same disk with a very low $\langle e\rangle = 6\times10^{-3}$, which permits efficient collisional accretion from km-scale bodies upward.

ever, by converting the collisional regime from an erosional state to an accretional state favoring accelerated growth. This is shown in the bottom panel of Fig. 8, which is a calculation using the same input disk as in the top panel of Fig. 8, but an $\langle e\rangle$ low enough to ensure efficient growth. If such low eccentricities were in fact extant early in the history of the solar system (e.g., before perturbations excited orbits in the disk or when significant nebular gas was still present), then the growth of larger objects would be promoted (owing in part to the gentler nature of collisions, and in part to the enhanced role of gravitational focusing at low relative velocities).

Determining whether a higher disk mass and/or lower

© American Astronomical Society • Provided by the NASA Astrophysics Data System

1995AJ....110..856S

disk eccentricities could have resulted in the growth of the QB_1's work requires the development of more sophisticated, time-dependent models that incorporate both velocity evolution and a complete representation of the accretion process. We are proceeding on the latter front now.

Before closing, however, it is useful to point out that the results obtained here suggest the intriguing possibility that the present-day Kuiper Disk shed considerable mass as it evolved through a more erosional stage reminiscent of the disks around the A stars β Pictorus, α PsA, and α Lyr. If so, our Kuiper Disk might be considered an older remnant of such a disk.

My colleagues Don Davis, Martin Duncan, Hal Levison, and Glen Stewart provided useful insights during this work. Paolo Farinella and Eli Dwek also provided helpful comments on an early version of this manuscript. This research was supported by the NASA Origins of Solar Systems Program.

REFERENCES

Bailey, M. E., & Stagg, C. R. 1990. Icarus 86, 2
Cochran, A. L., Levison, H. F., Stern, S. A., & Duncan, M. J. 1995, ApJ (in press)
Davis, D. R., *et al.* 1989, in Asteroids II, edited by R. P. Bizel, T. Gehrels, and M. S. Matthews (University of Arizona Press, Tucson), pp. 805–826
Duncan, M., Quinn, T., Tremaine, S. 1988. AJ, 94, L69
Duncan, M. J., Levison, H. F., & Budd, S. M. 1995, AJ, (submitted)
Edgeworth, K. E. 1949, MNRAS, 109, 600
Fernández, J. A. 1980, MNRAS, 192, 481
Fujiwara, A., et al. 1989, in Asteroids II, edited by R. P. Bizel, T. Gehrels, and M. S. Matthews (University of Arizona Press, Tucson), pp. 240–265
Holman, M. J., & Wisdom, J. 1993, AJ, 105, 1987
Jewitt, D., & Luu, J. X. 1993, Nature, 362, 730
Jewitt, D., & Luu, J. X. 1995, 109, 1867
Kuiper, G. P. 1951, in Astrophysics: A Topical Symposium, edited by J. A. Hynek (McGraw Hill, New York), pp. 357–424
Levison, H. F., & Duncan, M. J. 1993, AJ, 100, 1669
Lissaur, J. 1987, Icarus, 69, 249
Morbidelli, A., Thomas, F., & Moons, M. 1995, Icarus (submitted)
Petit, J.-M., & Hénon, M. 1987, A&A, 173, 389
Quinn, T. R. Tremaine, S., & Duncan, M. J. 1990, ApJ, 335, 667
Stern, S. A. 1988, Icarus, 73, 499
Stern, S. A. 1995a, in The Inventory of the Solar System, ASP Conf. Ser., edited by E. Bowell (in press)
Stern, S. A. 1995b, A&A (submitted)
Tremaine, S. 1990, in Baryonic Dark Matter, edited by D. Lynden-Bell and G. Gilmore (Kluwer, Dordrecht), pp. 37–65
Weissman, P. R. 1993, EOS, 74, 262

© American Astronomical Society • Provided by the NASA Astrophysics Data System